International Journal of Immunopathology & Pharmacology

Original Research

Cardioprotective effects of alantolactone on isoproterenol-induced cardiac injury and cobalt chloride-induced cardiomyocyte injury

International Journal of Immunopathology and Pharmacology
Volume 36: 1–18

DOI: 10.1177/20587384211051993
journals.sagepub.com/home/iji
SAGE

Miaomiao Liu[1], Panpan Liu[1], Bin Zheng[1], Yu Liu[1], Li Li[2], Xue Han[1], Yangshuang Liu[3] and Li Chu[1,4]

Abstract

Objectives: Alantolactone (AL) is a compound extracted from the roots of *Inula Racemosa* that has shown beneficial effects in cardiovascular disease. However, the cardioprotective mechanism of AL against hypoxic/ischemic (H/I) injury is still unclear. This research aimed to determine AL's ability to protect the heart against isoproterenol (ISO)-induced MI injury in vivo and cobalt chloride ($CoCl_2$) induced H/I injury in vitro.

Methods: Electrocardiography (ECG), lactate dehydrogenase (LDH), creatine kinase (CK), and cardiac troponin I (cTnI) assays in addition to histological analysis of the myocardium were used to investigate the effects of AL in vivo. Influences of AL on L-type Ca^{2+} current ($I_{Ca\text{-}L}$) in isolated rat myocytes were observed by the patch-clamp technique. Furthermore, cell viability, apoptosis, oxidative stress injury, mitochondrial membrane potential, and intracellular Ca^{2+} concentration were examined in vitro.

Results: The results indicated that AL treatment ameliorated the morphological and ECG changes associated with MI, and decreased levels of LDH, CK, and cTnI. Furthermore, pretreatment with AL elevated antioxidant enzyme activity and suppressed ROS production. AL prevented H/I-induced apoptosis, mitochondria damage, and calcium overload while reducing $I_{Ca\text{-}L}$ in a concentration and time dependent fashion. The 50% inhibiting concentration (IC_{50}) and maximal inhibitory effect (E_{max}) of AL were 17.29 μmol/L and 57.73 ± 1.05%, respectively.

Conclusion: AL attenuated MI-related injury by reducing oxidative stress, apoptosis, calcium overload, and mitochondria damage. These cardioprotective effects may be related to the direct inhibition of $I_{Ca\text{-}L}$.

Keywords

alantolactone, cardio-protection, oxidative stress, calcium influx, L-type calcium channel currents

Date received: 9 July 2021; accepted: 21 September 2021

[1]School of Pharmacy, Hebei University of Chinese Medicine, Shijiazhuang, China
[2]School of Pharmacy, Hebei Medical University, Shijiazhuang, China
[3]Integrative Medicine on Liver-Kidney Patterns, Institute of Integrative Medicine, College of Integrative Medicine, Hebei University of Chinese Medicine, Shijiazhuang, China
[4]Hebei Key Laboratory of Chinese Medicine Research on Cardio-Cerebrovascular Disease, Hebei University of Chinese Medicine, Shijiazhuang, China

Corresponding authors:
Yangshuang Liu, Integrative Medicine on Liver-Kidney Patterns, Institute of Integrative Medicine, College of Integrative Medicine, Hebei University of Chinese Medicine, 3 Xingyuan Road, Shijiazhuang 050200, Hebei, China.
Email: 957708622@qq.com.
Li Chu, School of Pharmacy, Hebei University of Chinese Medicine, 3 Xingyuan Road, Shijiazhuang 050200, Hebei, China.
Email: chuli0614@126.com.

Introduction

Myocardial ischemia (MI) is one of the cardinal pathological features of ischemic heart disease, which is the leading cause of death worldwide.[1] MI involves reduced blood perfusion of the heart, resulting in decreased oxygenation and aberrant energy metabolism that are insufficient to support healthy cardiac function.[2] Prolonged ischemia can lead to a point beyond which the cellular damages become irreversible and apoptosis becomes inevitable. Both oxidative stress and intracellular calcium overload have been implicated in MI.[3,4] The synergistic effects of oxidative stress and calcium overload induce cardiac cell dysfunction and apoptosis, which drastically impairs cardiac function.[5]

When the heart is subjected to hypoxia/ischemia (H/I), the concentration of calcium ions (Ca^{2+}) increases. An excessive increase in the intracellular calcium concentration would result in calcium overload and thus produce myocardial cell injury.[6,7] The Na^{+}/Ca^{2+} exchanger (NCX) is central to the mechanism of calcium efflux from cardiac myocytes.[8] Calcium is pumped out of the myocardial cell largely by the sarcolemmal NCX with some contribution from the sarcolemmal Ca-ATPase (PMCA).[9] These Ca^{2+} are located on the sarcoplasmic reticulum (SR) and the release of Ca^{2+} from the SR is termed "calcium-induced calcium-release."[10] In cardiomyocytes, L-type Ca^{2+} channels (LTCCs) are primarily responsible for the influx of Ca^{2+}, an essential intracellular messenger associated with the entire life cycle of this specialized cell type.[11] Inhibiting LTCCs results in reduced Ca^{2+} entry, and thus diminishes any Ca^{2+} overload. Reestablishing this Ca^{2+} homeostasis has a cardioprotective effect against MI injury.[12]

Augmented oxidative stress is one of the major elements of the complex pathophysiological mechanism underlying MI.[13] Oxidative stress results from the increased formation of reactive oxygen species (ROS) and causes DNA damage, protein and lipid peroxidation, and cellular dysfunction, all of which are associated with the pathological injury of the heart.[14] In most cell types, mitochondria are the primary source of ROS,[15] yet the damage ROS cause is not restricted to mitochondrial macromolecules but extends to the surrounding intracellular space as well.[16] Furthermore, ROS and mitochondria play important roles in apoptosis induction under both physiological and pathological conditions.[17] The most prevalent ROS include the peroxynitrite anion ($ONOO^{-}$), the superoxide anion radical (dioxide or O_2^{-}), and the hydroxyl radical (OH). Their high reactivity causes cellular dysfunction and sometimes cells death.[18] Myocardial injury causes excess production of ROS, and this oxidative stress leads to mitochondrial dysfunction and further aggravates cardiomyocyte apoptosis.[19] In the heart, mitochondria supply more than 90% of the adenosine triphosphate (ATP) required by the heart through oxidative phosphorylation.[20] Consequently, mitochondrial damage in MI due to oxidative stress causes excessive ROS production, dysfunction of mitochondria, and cellular injury.

Currently, natural products are an important resource for the development of small molecules for the treatment of various disease.[21] Alantolactone (AL, Desit, China; Figure 1) is a compound extracted from the roots of *Inula Racemosa* that exhibits a diversity of biological activities including anti-inflammatory, anti-cancer, anti-bacterial, and anti-fungal effects.[22] *Inula Racemosa* protects the heart from ISO-induced myocardial injury by reducing oxidative stress and modulating the hemodynamic and ventricular functions of heart.[23] In addition, *Inula Racemosa* exerts cardioprotective effects in ischemic rats and protects the myocardium of the rat heart from oxidative damage. However, the protective mechanism of AL in ischemic myocardial injury remains unknown.

Isoproterenol (ISO), a synthetic catecholamine, induces MI by increasing the force and frequency of myocardial contractions and raising intracellular Ca^{2+} concentration.[24] The ISO-induced MI model is not directly analogous to human occlusive MI, and this model may be more pertinent to MI which may involve excessive compensatory over-activity of the sympathetic nervous system.[25] The ISO-induced MI model is one of the most widely used experimental models to study the beneficial effects and cardiac functions of various drugs.[26] Cobalt chloride ($CoCl_2$) is a hypoxia-mimicking agent because of its property to mimic hypoxic/ischemic (H/I) conditions.[27] To model MI in vivo and H/I in vitro, in the present study, rats were injected with ISO and H9c2 cells were exposed to $CoCl_2$, respectively. The present study aimed to determine whether AL can play a protective role in the heart by reducing oxidative stress and regulating Ca^{2+} homeostasis.

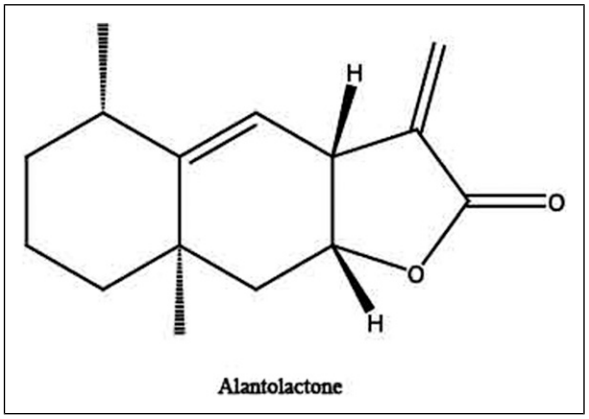

Figure 1. Chemical structure of alantolactone. (Molecular formula: $C_{15}H_{20}O_2$; Molecular weight, 232.32).

Materials and methods

Experimental animals and treatment

Adult male Sprague–Dawley (SD) rats (weigh: 200 ± 20 g; age: 8 weeks old) were supplied by the Laboratory Animal Center of Hebei Medical University. The rats were housed at 25 ± 1°C with 55 ± 5% humidity, on a 12 h light-dark cycle, and supplied with food and water. All procedures were carried out under the Guidelines of Animal Experiments from the Committee of Medical Ethics and approved by the Ethics Committee for Animal Experiments of Hebei University of Chinese Medicine (approval number: DWLL2020073).

Forty rats were evenly and randomly divided into four treatment groups (n = 10 rats per group): control (CON), isoprenaline (ISO), low dose AL group (L-AL), and high dose AL group (H-AL). The L-AL and H-AL groups received 25 and 50 mg/kg/d by oral gavage, respectively. Rats in the ISO and CON groups were gavaged with an equal volume of saline daily. After 7 days of continuous treatment, the rats in all but the CON groups were administered ISO (85 mg/kg) by subcutaneous injection on two consecutive days. After the final injection on day 9, the rats were deprived of food and water for 24 h. On day 10, electrocardiograms (ECGs) were performed, blood samples were collected, and the hearts were rapidly removed after administering anesthesia (sodium pentobarbital, 50 mg/kg according to body weight).

Detection of electrocardiogram (ECG), cardiac functional parameters, and cardiac marker enzymes

At the end of the experimental period, a standard limb leads II ECG was performed in rats. ECG recordings were obtained from the rats by using BL-420S experimental system. Catheterization of the left ventricle (LV) was performed on anesthetized rats after the final injection of ISO. A miniature pressure transducer was inserted into the aorta via the right carotid artery and advanced into the LV under continuous monitoring of the pressure waveform. LV systolic pressure (LVSP), LV end-diastolic pressure (LVEDP), and $\pm dp/dt_{max}$ were monitored continuously and then recorded and analyzed after 10 min of stabilization.

Sera were obtained by centrifuging the whole-blood samples. The levels of lactate dehydrogenase (LDH), creatine kinase (CK), and cardiac troponin I (cTnI) were measured using commercial kits according to the manufacturer's protocol (Nanjing Jiancheng Institute, China).

Histopathological examination of heart tissues

Heart tissue samples were fixed in 4% paraformaldehyde hydrated for 24 h before being embedded in paraffin. After standard hematoxylin and eosin (HE) staining, the sections of mid-myocardium (4 μm thick) were examined under a light microscope.

Immunohistochemistry

The tissue sections were dewaxed, rehydrated, and immersed in retrieval solution. Subsequently, the sections were treated with 3% hydrogen peroxide and incubated at 25°C for 20 min, and then washed in phosphate buffer solution (PBS) 3 times for 5 min each. Any non-specific staining was blocked with 5% Ig blocking reagent and 5% serum (Shanghai Regal Biological Technology Development Co., Ltd.) for 15 min at 37°C after rinsing. Slides were incubated with diluted rabbit polyclonal antibodies against TNF-α and IL-6 at 4°C overnight. The next day, the slides were rinsed 3 times with PBS for 5 min each. Next, the slides were incubated with their corresponding secondary antibodies for 20 min at room temperature. The target protein was then stained with 3,30-diaminobenzidine tetrahydrochloride.

Cell culture and experiment groups

H9c2 cells were cultured in high glucose Dulbecco's Modifed Eagle's Medium (DMEM, Gibco) supplemented with fotal bovine serum (FBS, Gibco) and antibiotics (1% penicillin-streptomycin, Gibco) in an atmosphere of 95% air and 5% CO_2 at 37°C. The medium was changed every 2–3 days. To select the appropriate concentration of AL, H9c2 cardiomyocytes were pretreated with AL at a range of concentrations (2.5, 5, 10, 20, and 40 μmol/L) for 24 h in untreated and $CoCl_2$-induced H9c2 cells. The cell viability assays suggested that AL had the most obvious survival pro-survival effect at about 10 μmol/L. Consequently, 5 and 10 μmol/L were chosen as the low and high doses for all subsequent experiments. The cells were classified into four groups: (1) CON (blank control of H9c2 cells); (2) $CoCl_2$ (H9c2 cells incubation with $CoCl_2$ (600 μmol/L)); (3) L-AL (H9c2 cells incubatd with $CoCl_2$ (600 μmol/L) and AL (5 μmol/L)); and (4) H-AL (H9c2 cells incubatd with $CoCl_2$ (600 μmol/L) and AL (10 μmol/L)). H9c2 myocytes in the CON group were cultured under normoxic conditions. The cells in the CoCl2 group were cultured with 600 μmol/L $CoCl_2$ for 24 h. The cells in the L-AL and H-AL groups were pretreated with 5 and 10 μmol/L AL for 24 h, respectively, followed by incubation with 600 μmol/L $CoCl_2$ for 24 h.

Detection of cell viability

The effect of AL on cell viability was evaluated using the Cell Counting Kit-8 (CCK-8, Biosharp, China) assay. H9c2 cells were seeded in 96 well cell culture plates 1×10^4 cells/

well. After the aforementioned treatments, a solution of 10 μL of CCK-8 diluted in 100 μL DMEM was added to each incubated for 2 h at 37°C. The OD at 450 nm was measured using a microplate reader (Thermo, USA).

Detection of LDH and CK release in culture medium

Cellular injury was assessed by LDH and CK release. H9c2 cells were cultured at 1×10^6 cells/well in six well plates. The cell culture medium was collected after the cell viability experiment (described above). The contents of LDH and CK were quantified using commercial kits according to the manufacturer's instructions (Nanjing Jiancheng Institute, China).

Evaluation of cell apoptosis using Hoechst-33258 staining and flow cytometry

Following treatment, the cells from each group were washed with cold PBS and incubated with Hoechst 33342 dye for 15 min in the dark at room temperature. Hoechst fluorescence was visualized and imaged using a fluorescence microscope (Olympus, Japan).

The rate of apoptosis among H9c2 cardiomyoblasts was detected using Annexin V-FITC/PI Apoptosis Kit in accordance with the manufacturer's instructions. The cells from the four treatment groups were collected and washed 3 times with PBS before being resuspended in a prepared binding buffer (100 μL). The cell suspensions were transferred into a 5 mL flow tube and stained with 5 μL Annexin V-FITC/PI that incubate at room temperature for 15 min in the dark. Finally, the cells were analyzed using a flow cytometer.

Measurement of intracellular superoxide dismutase (SOD), catalase (CAT), glutathione (GSH), and malondialdehyde (MDA)

H9c2 cells were cultured at a density of 1×10^6 cells/well in six well plates. Then, H9c2 cells were washed with cold PBS, and centrifuged at 14,000 r/5 min. The supernatant was removed and the precipitate was sonicated and the H9c2 cell lysate was resuspended. The activities of CAT, SOD, MDA, and GSH were analyzed using commercial kits (Nanjing Jiancheng Institute, China).

Measurement of intracellular ROS production

ROS production was assessed with the peroxide-sensitive fluorescent probe 2′,7′-dichlorofluorescin in diacetate (DCFH-DA). The dye was loaded by incubating the H9c2 cells with 20 μmol/L DCFH-DA for 15–20 min at 37°C. The cells were then visualized imaged using a fluorescence microscope (Olympus, Japan).

Measurement of Mitochondrial membrane potential (MMP)

Rhodamine 123 was used to estimate the electrical potential across the inner mitochondrial membrane. Following the experimental treatments, H9c2 cells were washed with PBS and incubated with rhodamine 123 for 15 min at 37°C. Subsequently, the cells were washed with PBS twice, and images were captured with a fluorescence microscope (Olympus, Japan).

Determination of intracellular Ca^{2+} concentration

To determine the intracellular Ca^{2+} concentration, H9c2 cardiomyocytes were incubated with Fluo-3/AM in the dark for 20 min. Then, the cells were visualized and imaged by using a fluorescence microscope (Olympus, Japan).

Isolation of rat ventricular myocytes

To obtain normal cardiomyocytes, rats were injected with heparin (500 IU/kg) intraperitoneally and then anesthetized with ethyl carbamate (1.0 g/kg) 20 min later. The hearts were then rapidly excised and perfused for 5 min at a rate of 4 mL/min via the aorta with oxygenated ice-cold Ca^{2+}-free Tyrode's solution (NaH_2PO_4 0.33 mM, $MgCl_2$ 1.0 mM, KCl 5.4 mM, glucose 10 mM, HEPES 10 mM, and NaCl 135 mM, pH 7.4). The heart was retrogradely perfused with an enzymatic solution containing Ca^{2+}-free Tyrode's solution with $CaCl_2$ (34 μmol/L), and collagenase type II (500 mg/L) using Langendorff equipment for 15–20 min. Subsequently, the hearts were washed with Tyrode's solution after the enzymatic digestion. The heart was cut into small pieces and kept in an oxygenated Krebs buffer (KB) solution (EGTA 1 mM, $MgSO_4$ 3 mM, glucose 10 Mm, HEPES 10 mM, taurine 20 mM, KH_2PO_4 25 mM, KCl 40 mM, L-glutamic acid 50 mM, and KOH 80 mM, pH 7.2). The ventricular myocytes were incubated for 1 h at room temperature.

To obtain ischemic cardiomyocytes, rats were injected with ISO subcutaneously (85 mg/kg). After treatment with ISO, the hearts were excised as described above to isolate the cardiomyocytes.

Electrophysiology

The Ca^{2+} current was detected in rat ventricular myocytes using a whole-cell patch-clamp technique. The whole-cell configuration was maintained at a room temperature using a glass pipette with a tip resistance of 2–5 MΩ filled with

pipette solution (TTX 10 μM, $CaCl_2$ 1.8 mM, $MgCl_2$ 2.0 mM, glucose 10 mM, HEPES 10 mM, and TEA-Cl 140 mM, PH 7.4), and 50–70% series resistance compensation was achieved. For all drug applications, we used a small bath volume and fully exchanged the external solution. The cells were suspended in the external solution ($MgCl_2$ 0.5 mM, $CaCl_2$ 2.5 mM, CsCl 5.4 mM, HEPES 5.5 mM, glucose 11 mM, and NaCl 140 mM, pH 7.4). AL was dissolved in dimethyl sulfoxide (DMSO) and diluted in the external solution to achieve concentrations of 0.3, 1, 3, 10, and 30 μmol/L. The maximum percent of DMSO in final experimental test solutions was 1%.

For all experiments, the holding potential was −80 mV followed by depolarization to 0 mV. Meanwhile, the Ca^{2+} currents were elicited by a 200 msec depolarizing pulse. Membrane capacitance (C_m) was estimated from capacitive transients and calculated according to $C_m = \tau_m \times I_o V_m (1 - I_{ss}/I_o)$, where τ_m is the membrane time constant, I_o is the maximal amplitude of the capacitive current spike, I_{ss} is the current at the end of the 10 msec pulse (steady state), and V_m is the amplitude of the voltage step (C_m = 152.8 ± 23.7 pF). Axon patch 200B amplifier and pClamp 10.2 software (Axon Instruments, Union City, CA, USA) were used to record the currents.

Statistical analysis

All data were analyzed and fitted b using Origin 7.5 (OriginLab Corp., Northampton, USA) and Clampfit 10.2 software (Molecular Devices, Sunnyvale, USA) software. The inhibition ratio of AL on $I_{Ca\text{-}L}$ was calculated $(I_{Control} - I_{Drug})/I_{Control}$. The concentration-response curve was fit with the logistic equation: $y = A_2 + (A_1 - A_2)/[1 + (x/x_0)^p]$, where p is the Hill coefficient, A_1 is the maximum responses, A_2 is the minimum responses, and x is the drug concentration and y is the response. The steady-state activation and inactivation curves of $I_{Ca\text{-}L}$ were fit with Boltzmann functions: $y = A/\{1 + \exp[(V_h - V_m)/k]\}$, where A is the amplitude of the relationship, k is the slope, V_m is the test potential, and V_h is the voltage at half-maximal activation.

All data are presented as mean ± standard error of the mean (SEM). Comparisons were made via one-way analysis of variance (ANOVA) followed by Tukey's post hoc test. $p < 0.05$ was considered reflective of statistical significance.

Results

Effects of AL on ECG, cardiac functional parameters, and cardiac marker enzymes

The needle electrode was inserted subcutaneously between the paw pads of each rat and the ECG was recorded continuously. Compared with the CON group, the ST interval increased, and the amplitude of the R wave decreased in the ISO-induced group (Figure 2(a)–(c)). The L-AL and H-AL groups showed ST interval and R wave amplitude recovery. As shown in Table 1, ISO treatment caused significant increases ($p < 0.01$) in LVEDP compared with the CON group. On the other hand, ISO caused significant decreases in LVSP and ± dp/dt_{max} compared to the CON group. Table 1 shows that AL pretreatment restored both parameters to nearly baseline levels ($p < 0.01$).

As shown in Figure 2(e)–(g), the levels of LDH, CK, and cTnI, heart rate, and J-point elevation were increased in the ISO group, indicated that the model of MI in this research was successfully established ($p < 0.01$). Compared with the ISO group, J-point elevation, heart rate, and LDH, CK, and cTnI levels in the L-AL and H-AL groups were decreased ($p < 0.01$).

Effects of AL on histopathology

The myocardial tissue structure in the CON group was clear, myocardial cell arrangements were orderly, the cell membrane was intact, the nucleus was clear, and no pathological change was observed. As shown in Figure 2(d), the heart tissues from ISO-induced MI rats exhibited obvious interstitial edema, inflammatory cell infiltration and either pyknotic or deepening nucleus, the results are consistent with previous study.[28] In contrast, the L-AL and H-AL groups showed clear transverse striations, indicating that pretreatment with AL suppressed the ISO-induced myocardial pathology.

Effects of AL on IL-6 and TNF-α expression levels

The expression levels of IL-6 and TNF-α in cardiac tissue were assessed using immunohistochemistry. As shown in Figure 3, IL-6 and TNF-α expression were low in the CON group and increased after ISO treatment. AL pretreatment reversed these inflammatory expressions. The expression of inflammation in L-AL and H-AL groups was significantly lower than that in the ISO group.

Effects of AL on cell viability

We analyzed the viability of H9c2 cells treated with different concentrations of AL using the CCK-8 assay (Figure 4). Incubating H9c2 cells with increasing concentrations of $CoCl_2$ (400–800 μmol/L) significantly reduced their viability ($p < 0.01$, $p < 0.05$). Figure 4(b) displayed that 2.5, 5, 10, and 20 μmol/L AL treatment not significant effect on H9c2 cell viability. AL concentrations of 5 and 10 μmol/L were selected for all further experiments. Compared with CON group, exposure to $CoCl_2$ for 24 h reduced the growth of H9c2 cells ($p < 0.01$, $p < 0.05$). However, pretreatment with AL significantly increased the viability of H9c2 cells ($p < 0.01$).

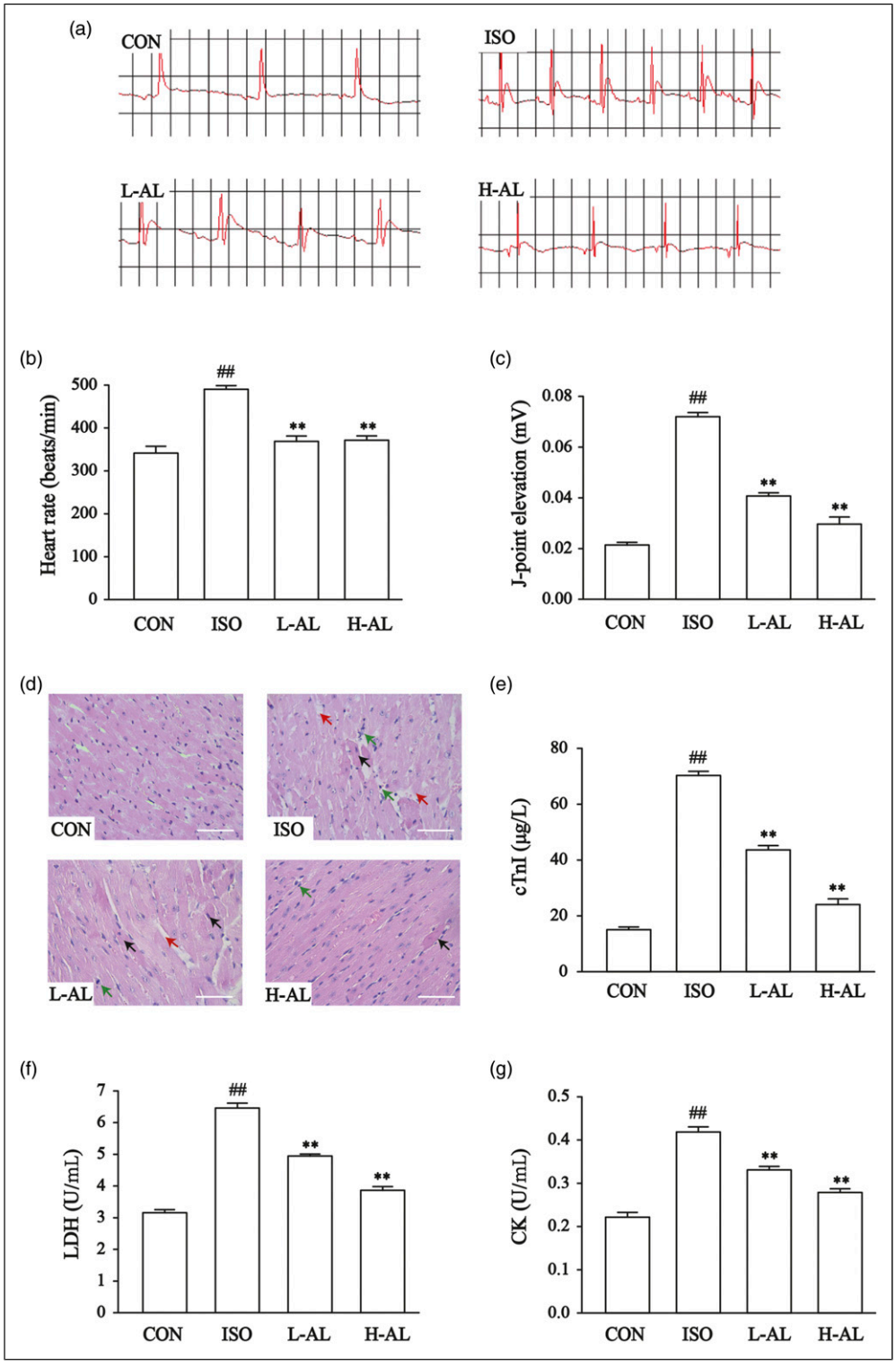

Figure 2. Effects of AL on ECG, histopathology, and cardiac enzymes. (a) Representative ECG tracings. (b and c) Statistical analysis of heart rate and J-point elevation. (d) Representative microscopic photographs of hearts stained with H&E (magnification: ×400, Scale bar: 50 μm). Those arrows distinguish clearly for edema (red arrow), inflammatory cell infiltration (green arrow), and either pyknotic or deepening nucleus (black arrow). (e–g) cTnI, LDH and CK levels in serum. The values are the means ± SEM (n = 10, $^{\#\#}p < 0.01$ vs CON; $^{**}p < 0.01$ vs ISO).

Table 1. Effects of AL on changes of cardiac functional parameters.

Group	LVEDP (mmHg)	LVSP (mmHg)	+dp/dt$_{max}$ (mmHg/s)	-dp/dt$_{max}$ (mmHg/s)
CON	5.24 ± 0.15	156.64 ± 9.74	6057.72 ± 143.66	5531.85 ± 169.22
ISO	21.12 ± 1.34$^{\#\#}$	102.71 ± 10.65$^{\#\#}$	3410.80 ± 155.54$^{\#\#}$	3196.03 ± 141.24$^{\#\#}$
L-AL	14.68 ± 0.45*	121.46 ± 14.95*	4565.01 ± 63.52**	4728.22 ± 180.10**
H-AL	7.16 ± 0.42**	139.12 ± 11.77**	5486.20 ± 133.72**	5108.72 ± 216.46**

The values are the means ± SEM ($^{\#}p < 0.05$ vs CON; $^{\#\#}p < 0.01$ vs CON; $^{*}p < 0.05$ vs ISO; $^{**}p < 0.01$ vs ISO).

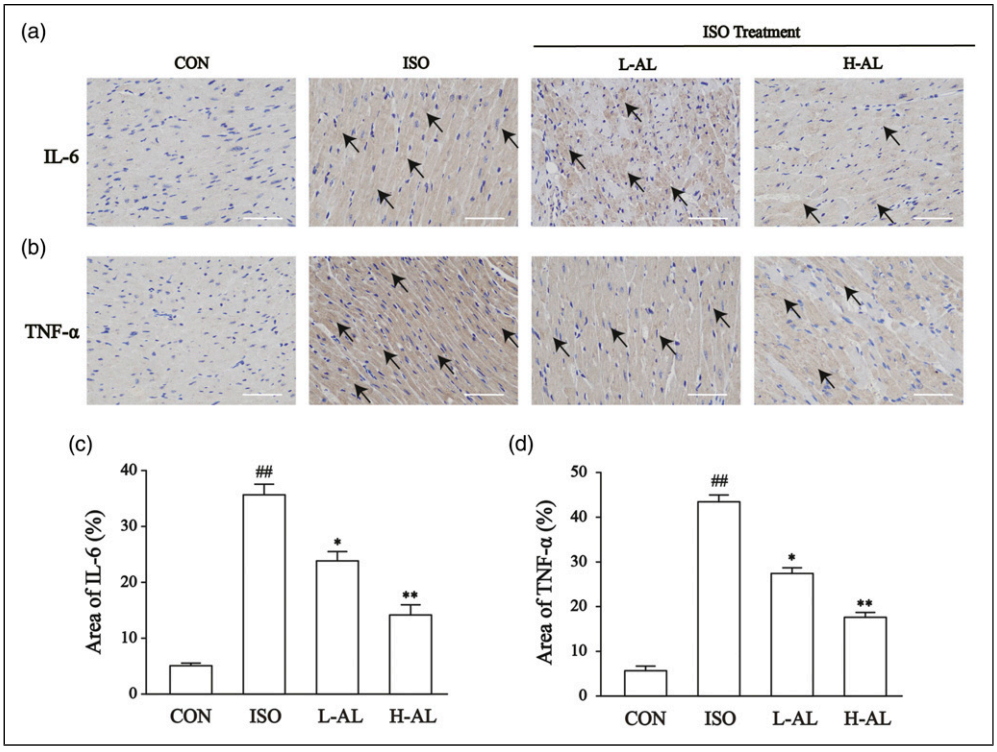

Figure 3. Effects of AL on IL-6 and TNF-α expression as detected by immunohistochemistry. Heart tissues were obtained from the CON, ISO, L-AL, and H-AL groups. The morphological location and area percentages of IL-6 expression (a and c), and TNF-α expression (b and d) are shown. Magnification: ×400, scale bar: 50 μm. Positive expression of IL-6, and TNF-α is shown by arrows. The values are the means ± SEM ($^{\#\#}p < 0.01$ vs CON; $^{*}p < 0.05$ vs ISO; $^{**}p < 0.01$ vs ISO).

Effects of AL on LDH and CK activities in culture medium

As shown in Figure 5(c) and (d), the enzymatic activities of LDH and CK increased in the $CoCl_2$ group compared with the CON group ($p < 0.01$). The activities of LDH and CK present in the culture medium decreased when AL pretreatment preceded the addition of $CoCl_2$ ($p < 0.01, p < 0.05$).

Effects of AL on apoptosis

Compared with the CON group, apoptosis among the cells in the $CoCl_2$ group had dramatically increased ($p < 0.01$). After being treated with $CoCl_2$ for 24 h, the H9c2 cells presented with condensed and fragmented nuclei and apoptotic bodies (Figure 5(a) and (b)). Pretreatment with 5 and 10 μmol/L AL for 24 h before $CoCl_2$ addition reduced the number of apoptotic cells significantly ($p < 0.01$).

Figure 5e shows the effects of AL on apoptosis as detected by flow cytometry. These results evidenced that the apoptosis rate of the $CoCl_2$ group was significantly increased relative to the CON group. However, the apoptosis rate of the AL treatment group was significantly lower than the $CoCl_2$ group ($p < 0.01$).

Effects of AL on oxidative stress

DCFH-DA was employed to evaluate ROS levels in H9c2 cells.[29] As shown in Figure 6(a) and (b), in contrast to the CON group, the amount of ROS in the $CoCl_2$ group increased significantly ($p < 0.01$). Pretreatment with AL decreased intracellular ROS generation in H/I-induced

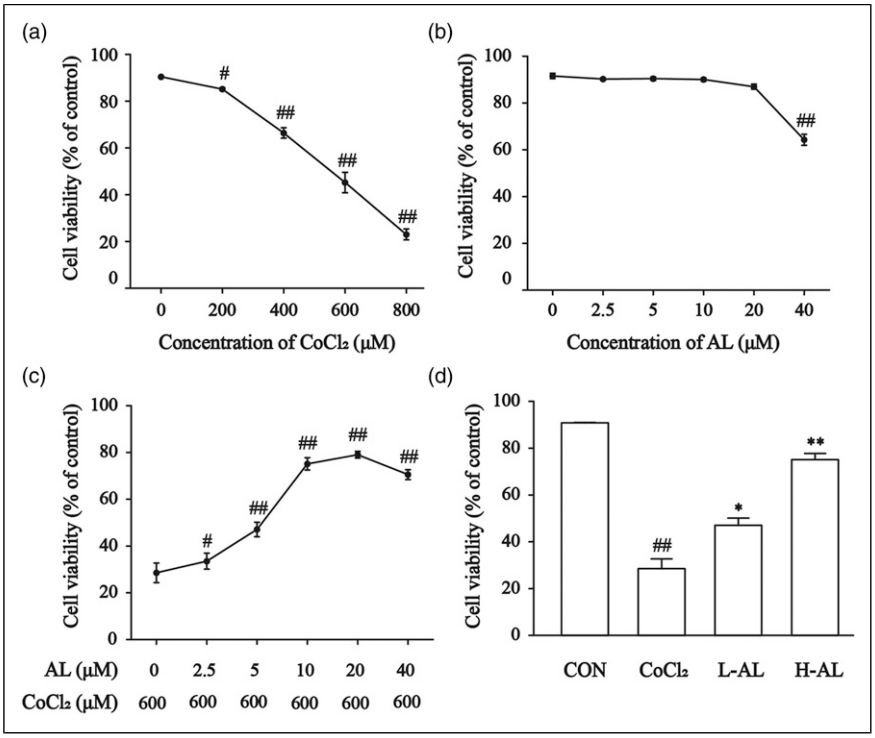

Figure 4. Effects of AL on H9c2 cell viability. (a) Cell viability was measured following treatment with $CoCl_2$ (0–800 μmol/L). (b) Cell viability of H9c2 cell was measured following treatment with AL (2.5, 5, 10, 20 and 40 μmol/L). (c and d) Cell viability of H9c2 cell was measured following treatment with AL and $CoCl_2$. The values are the means ± SEM (n = 6, $^{\#}p < 0.05$ vs CON; $^{\#\#}p < 0.01$ vs CON; $^{*}p < 0.05$ vs $CoCl_2$; $^{**}p < 0.01$ vs $CoCl_2$).

cardiomyocytes ($p < 0.01$). These findings suggested that AL pretreatment prevents $CoCl_2$-induced oxidative stress in cardiomyocytes. As shown in Figure 6(c)–(f), $CoCl_2$ caused significant decreases in the activities of CAT, GSH and SOD compared with the CON group ($p < 0.01$). Pretreatment with AL significantly increased the levels of CAT, GSH, and SOD compared with the $CoCl_2$ group ($p < 0.01$). Additionally, treatment with $CoCl_2$ along increased the MDA concentration relative to control, and AL pretreatment prevented this effect ($p < 0.01$).

Effects of AL on mitochondrial membrane potential (MMP)

The change of rhodamine 123 fluorescence to examine whether preservation of MMP is associated with cardioprotective effects of AL was assessed. The MMP in the $CoCl_2$ group was downregulate compared with the CON group ($p < 0.01$). Meanwhile, the MMP was elevated significantly in the L-AL and H-AL groups, in contrast to the $CoCl_2$ group (Figure 7(a) and (c)) ($p < 0.01$, $p < 0.05$).

Effects of AL on Ca^{2+} concentration

To determine the intracellular Ca^{2+} concentration of H9c2 cells, we quantified the ratio of Fura-3/AM staining. The result indicated that intracellular Ca^{2+} accumulation was increased in $CoCl_2$-treated H9c2 cells ($p < 0.01$). The intensity of Ca^{2+} fluorescence dramatically decreased in H9c2 cells after pretreatment with 5 and 10 μmol/L AL (Figure 7(b) and (d)) ($p < 0.01$).

Confirmation of $I_{Ca\text{-}L}$

As shown in Figure 8(a) and (b), as a specific T-type Ca^{2+} channel blocker, $NiCl_2$ (0.01 mmol/L) did not affect the inward currents, which demonstrated that the induced currents were not mediated by T-type Ca^{2+} channels. VER (1 μmol/L) is a specific LTCC blocker that attenuated the current almost entirely, indicating that these currents were $I_{Ca\text{-}L}$.

Effects of AL on $I_{Ca\text{-}L}$

Figure 9(a)–(f) shows the reversible Ca^{2+} current recording after the effective dose of 10 μmol/L AL was added both in healthy and ischemic cardiomyocytes. AL reduced $I_{Ca\text{-}L}$ with an inhibition rate of 42.62 ± 5.18% and 44.14 ± 4.56%, respectively. After washing out with external solution, the currents partially recovered. These results speak to the reversibility of AL's effects on $I_{Ca\text{-}L}$.

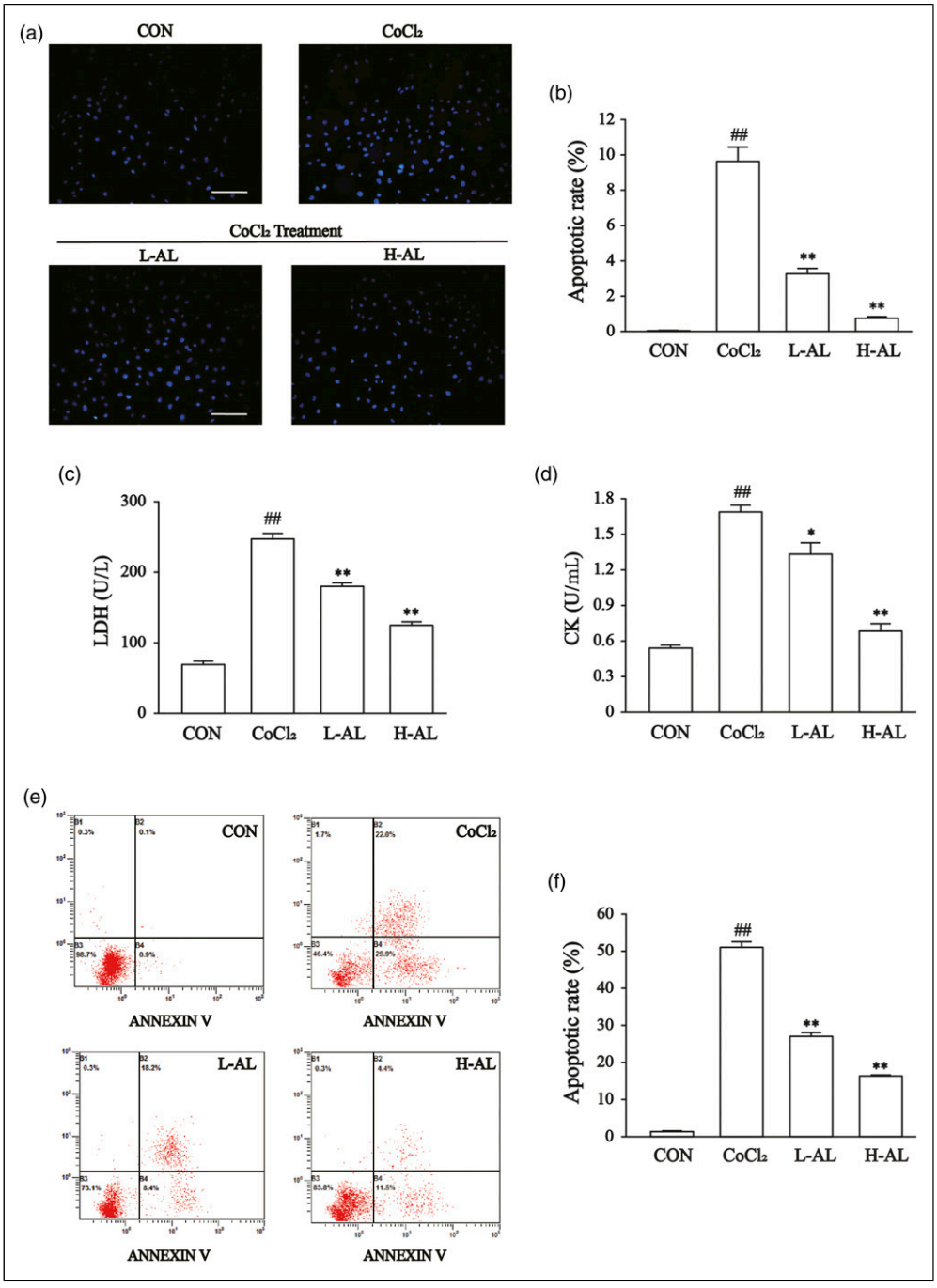

Figure 5. Effects of AL on apoptosis and cardiac marker enzymes. (a and b) The morphological changes of H9c2 cells are shown by Hoechst-33258 staining (magnification: ×200, Scale bar: 100 μm). (c and d) LDH and CK levels in cell culture supernatant. (e and f) Apoptosis rates were determined using flow cytometry. The values are the means ± SEM ($n = 6$, $^{\#\#}p < 0.01$ vs CON; $^{*}p < 0.05$ vs $CoCl_2$. $^{**}p<0.01$ vs $CoCl_2$).

Concentration-dependent effects of AL on $I_{Ca\text{-}L}$

Figure 9(g)–(i) contains representative traces for a range of AL concentrations. With increasing concentrations of AL (from 0.3 to 30 μmol/L), $I_{Ca\text{-}L}$ was gradually suppressed. The peak amplitude of $I_{Ca\text{-}L}$ was reduced by 2.25 ± 0.17%, 12.70 ± 0.71%, 22.91 ± 1.12%, 42.78 ± 1.06%, and 57.73 ± 1.05% by AL derivatives at 0.3, 1, 3, 10, and 30 μmol/L, respectively, and the 50% inhibiting concentration (IC_{50}) of AL was 17.29 μmol/L. Effects of AL on the current–voltage (I–V) relationship of $I_{Ca\text{-}L}$.

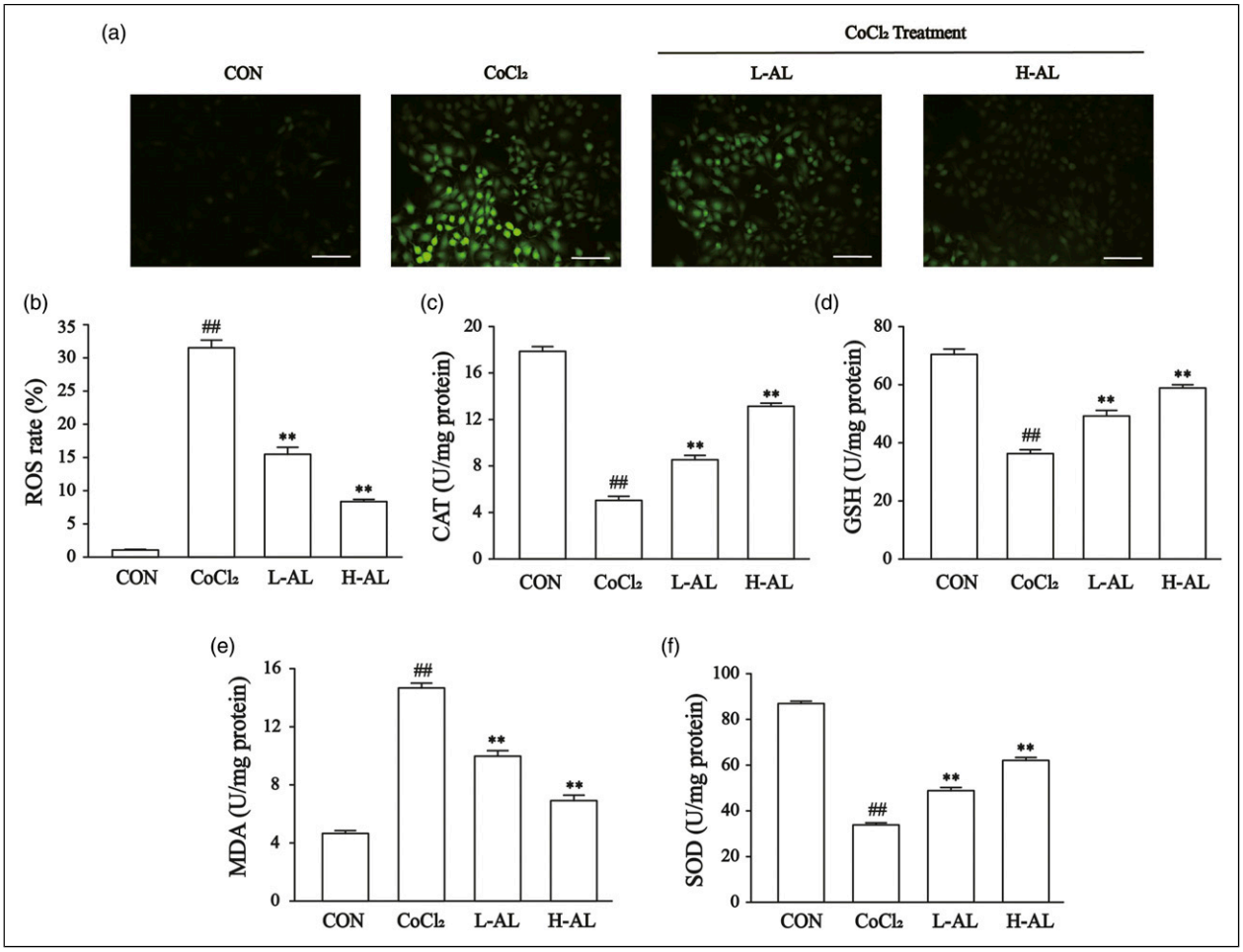

Figure 6. Effects of AL on $CoCl_2$-induced oxidative stress in H9c2 cells. (a and b) Intracellular oxidant stress evaluation with 2′,7′-dichlorofluorescin diacetate (DCFH-DA) labeling in H9c2 cells (magnification: ×200, Scale bar: 100 μm). (c–f) MDA content, and the activities of SOD, CAT, and GSH were measured in H9c2 cardiomyocytes. The values are the means ± SEM ($n = 6$, $^{\#\#}p < 0.01$ vs CON; $^{**}p < 0.01$ vs $CoCl_2$).

As shown in Figure 10(a) and (b), the effects of AL (3 μmol/L and 10 μmol/L) on the I–V relationship are depicted. The I–V curves showed an upward trend. The $I_{Ca\text{-}L}$ amplitude increased from −20 mV and attained a maximum at 0–10 mV. These results demonstrated that AL 3 and 10 μmol/L reduced the maximum current by a significant margin.

Effects of AL on steady-state activation and inactivation of $I_{Ca\text{-}L}$

Figure 10(c) and (d) shows that both concentrations of AL (3 and 10 μmol/L) affected the steady-state activation and inactivation of $I_{Ca\text{-}L}$. The mean half-maximum activation voltage ($V_{1/2}$) value of activated $I_{Ca\text{-}L}$ in the CON group was –11.60 ± 0.66 mV, and the slope factor (k) was 4.56 ± 0.62 mV. However, compared with the CON group, the values of $V_{1/2}$ for activation with 3 μmol/L of AL was –12.84 ± 0.47 mV and the k value was 4.23 ± 0.40 mV. The values of $V_{1/2}$ for activation with 10 μmol/L of AL were −13.45 ± 0.16 mV and the k value was 4.59 ± 0.13 mV. Without AL, $V_{1/2}$ of inactivation was –24.30 ± 0.47 mV and the k value was 4.93 ± 0.39 mV. In the presence of 3 and 10 μmol/L AL, the values of $V_{1/2}$ for inactivation were –26.95 ± 0.28 mV and –29.99 ± 0.57 mV, respectively, and the k values were 3.69 ± 0.22 mV and 4.37 ± 0.60 mV, respectively.

Discussion

The present study revealed several major findings: (1) AL protected ISO-induced against myocardial damage in vivo; (2) AL effectively reduced $CoCl_2$-induced apoptosis, oxidative stress, mitochondrial damage, and calcium overload in vitro; and (3) the cardioprotective effects of AL via the direct inhibition of $I_{Ca\text{-}L}$ in rat ventricular myocytes. To our

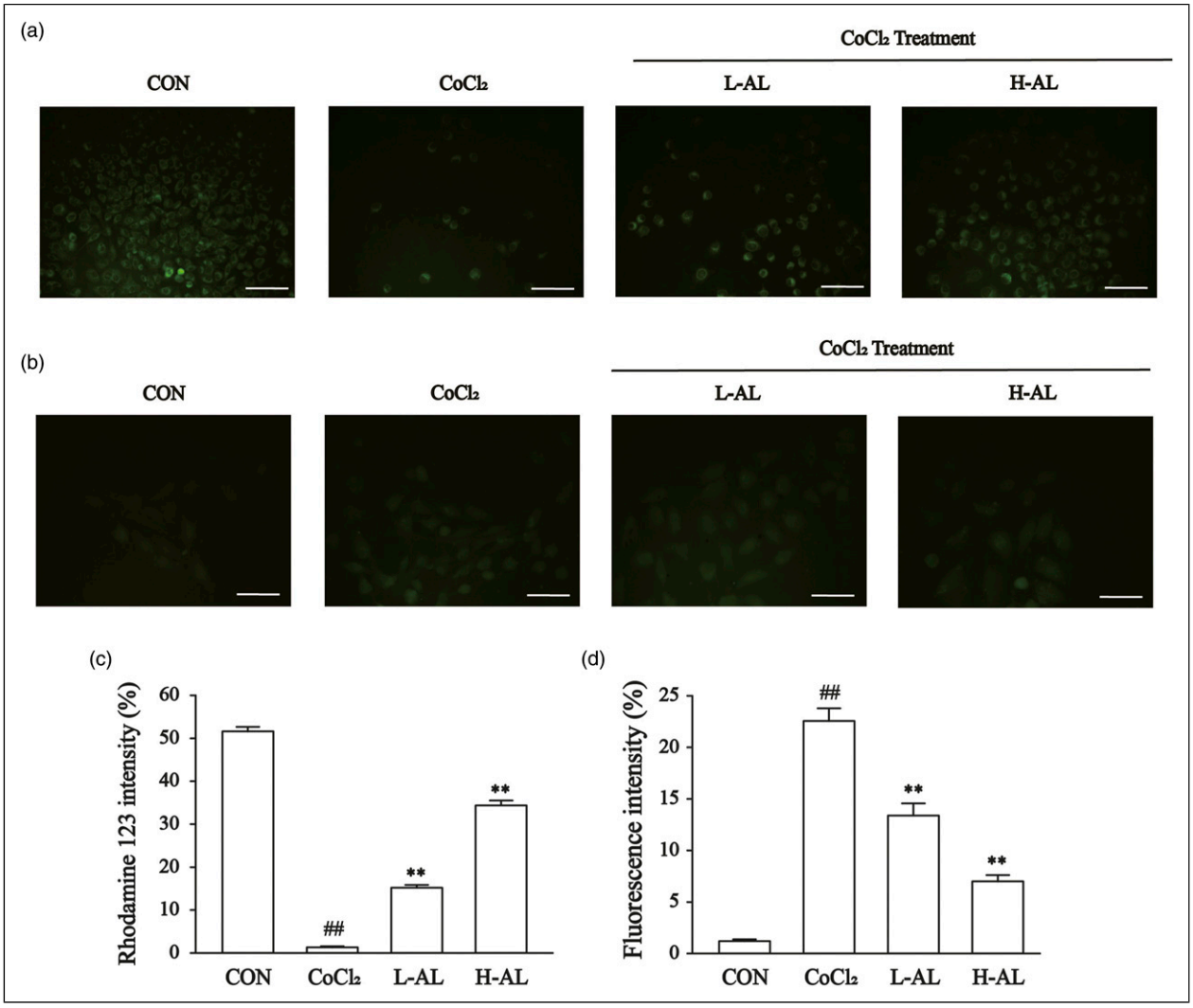

Figure 7. Effects of AL on mitochondrial membrane potential and Ca^{2+} concentration in H9c2 cells. (a) Representative image of rhodamine 123 fluorescence intensity in H9c2 cells (magnification: ×200, Scale bar: 100 μm). (b) Representative image of intracellular Ca^{2+} concentration fluorescence intensity in H9c2 cells (magnification: ×400, Scale bar: 50 μm). (c and d) Statistical analysis of rhodamine 123 and intracellular Ca^{2+} concentration fluorescence intensities, respectively. The values are the means ± SEM (n = 6, $^{\#\#}p < 0.01$ vs CON; $^{**}p < 0.01$ vs $CoCl_2$).

knowledge, this is the first study to investigate the mechanism of AL to protect the heart against ischemic injury.

AL has been used as one of the main components of Guanxinsuhe capsules (GXSHC). GXSHC can protect H_2O_2 injured cardiomyocytes by increasing their antioxidant capability.[30] Meanwhile, GXSHC treats myocardial infarction by regulating troponin.[31] Taken together, these studies indicate that GXSHC has a protective effect on the heart. However, little is known regarding whether AL can protect against myocardial disease. The findings described in the present study support the cardioprotective effect of AL against MI injury.

The pathophysiological mechanisms of MI are complex and have a profound impact on the global burden of heart disease.[32] Unlike in other tissues and muscles subtypes, cardiac metabolism is almost entirely aerobic. Therefore, the perfect balance between myocardial oxygen consumption and myocardial oxygen supply is necessary for maintaining ventricular function and avoiding MI.[33] ISO is often used to model MI in experimental animals because it induces ischemia, hypoxia, Ca^{2+} overload, and depletes energy reserves.[34]

Examination of the ECG, LV function, and histology in rats treated with ISO showed myocardial cell damage, depressed systolic pressure, and increased LVEDP, leading to MI. Compared with the CON group, subcutaneous injection of ISO-induced MI as indicated by tachycardia and J-point elevation. Pretreatment with AL could decrease

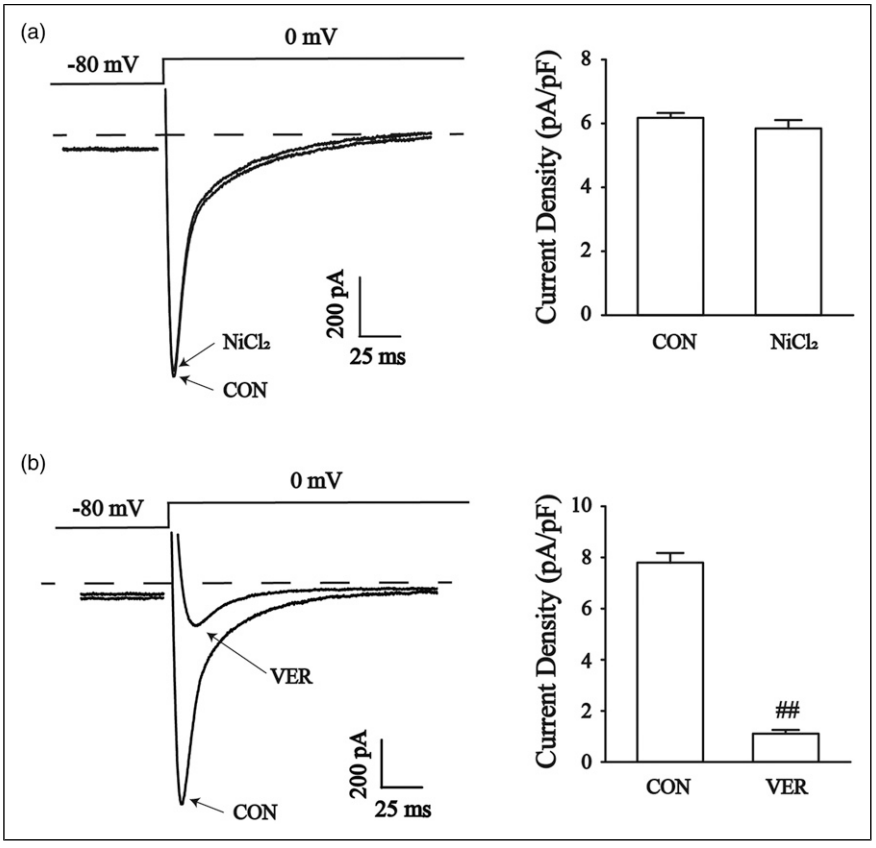

Figure 8. Confirmation of $I_{Ca\text{-}L}$ in myocardial cells. (a) Representative trace recorded after treatment with $NiCl_2$ (0.01 mM). (b) Representative trace after treatment with VER (1 μM). The values are the means ± SEM (n = 6, $^{\#\#}p < 0.01$ vs CON).

heart rate and J-point. Compared with the parameters in the ISO group, LVEDP decreased while LVSP and ± dp/dt_{max} significantly increased in the H-AL and L-AL groups. The evaluation of CK and LDH levels has been the gold standard for the enzymatic diagnosis of acute MI. cTnI is a polypeptide involved in myocardial contraction and is a highly sensitive biomarker of myocardial injury. In the ISO group, the levels of CK, LDH, and cTnI remarkably increased compared with the CON group. Pretreatment with AL caused the levels of CK, LDH, and cTnI to decrease.[35] Meanwhile, HE-stained sections confirmed that the heart tissue of the model group was markedly injured. Tissue from the ISO group exhibited infiltrating inflammatory cells, widened muscle space, and striation loss with nuclear changes. The damage observed in the H-AL and L-AL groups was reduced compared with the ISO group. In the present study, the mechanism underlying the myocardial protection conferred by AL was investigated by analyzing the expression levels of pro-inflammatory markers. ISO induced a significant increase in IL-6 and TNF-α expression. However, AL treatment decreased these elevated pro-inflammatory factor expression levels. Taken together, these data describe the ability of AL pretreatment to prevent the changes associated with this specific disease state.

$CoCl_2$-treated H9c2 cells represent a robust in vitro model for exploring the mechanisms of H/I-related damage, since H9c2 cells exhibit the biochemical and electrophysiological characteristics of cardiomyocytes.[36] The H9c2 cell line has been established from embryonic rat cardiac ventricle and it has properties similar to neonatal and adult cardiomyocytes, which can functionally express LTCCs of cardiac.[37] In the current study, $CoCl_2$ was used to mimic H/I-induced apoptosis in H9c2 cardiomyocytes. Myocardial cell apoptosis is an important pathological process in H/I-induced myocardial injury, which is closely related to cardiac insufficiency. According to the CCK-8 results, cardiomyocyte viability decreased following treatment with $CoCl_2$, and the apoptosis rate increased. In apoptotic cells, intracellular LDH and CK are released through damaged cell membrane structures. Therefore, it is an indirect method to evaluate H9c2 cell injury by detection of LDH and CK concentration. Levels of the indicators used for MI diagnosis, CK and LDH were significantly increased after treatment with $CoCl_2$. Importantly, we found that 5 and 10 μmol/L AL protected H9c2 cells against $CoCl_2$-induced injury, enhancing cell viability and decreasing the levels of LDH and CK. In addition, the flow cytometry and apoptotic fluorescence results show that the

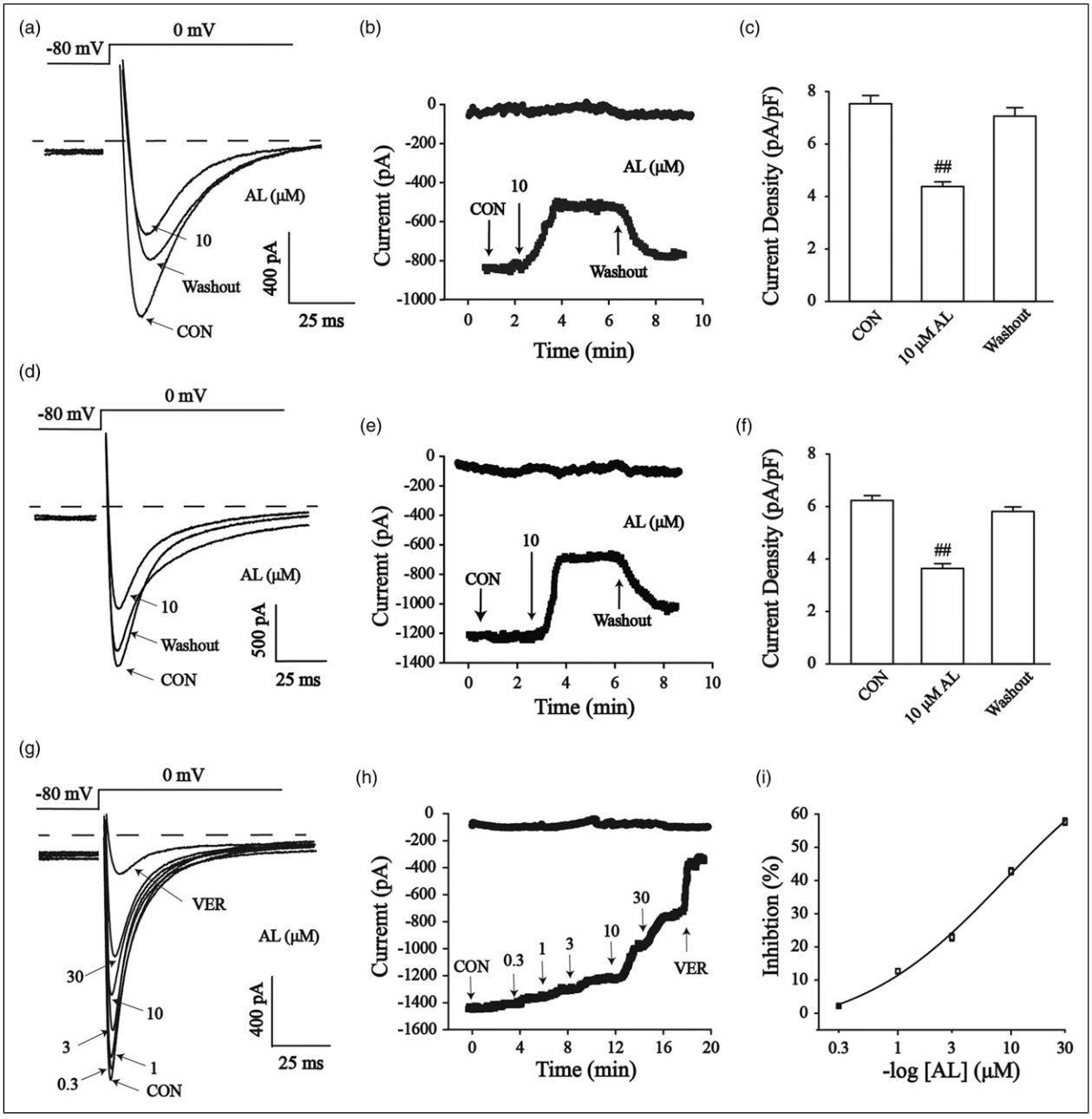

Figure 9. The reversible effect of AL on $I_{Ca\text{-}L}$. (a–c) Healthy and (d–f) ischemic ventricular myocytes in rats. (g) Exemplary traces and (h) time course of $I_{Ca\text{-}L}$ were recorded under control conditions during exposure to 0.3, 1, 3, 10, and 30 μM AL, or 1 μM VER. (i) Concentration-response curves representing the percent inhibitory effects of AL. The values are the means ± SEM (n = 6, $^{\#\#}p < 0.01$ vs CON).

AL treated groups exhibited decreased apoptosis rates, which supports the protective effect of AL against $CoCl_2$-induced apoptosis.

Increased production of ROS and ROS-mediated oxidative damage during the MI process play crucial roles in the development of H/I injury. When ROS accumulate continuously and the endogenous antioxidant defense system cannot clear these in a timely fashion, oxidative stress is induced.[38] The cytotoxicity induced by $CoCl_2$ is due to the increased production of free radicals (including ROS) mediated by hypoxia. The balance between the production of ROS and the elimination of excess ROS is essential to maintain the redox state and homeostasis in cells. Compared with the control cells, the $CoCl_2$ treated cells exhibited significantly increased production of ROS. Our results showed that pretreatment with 5 and 10 μmol/L

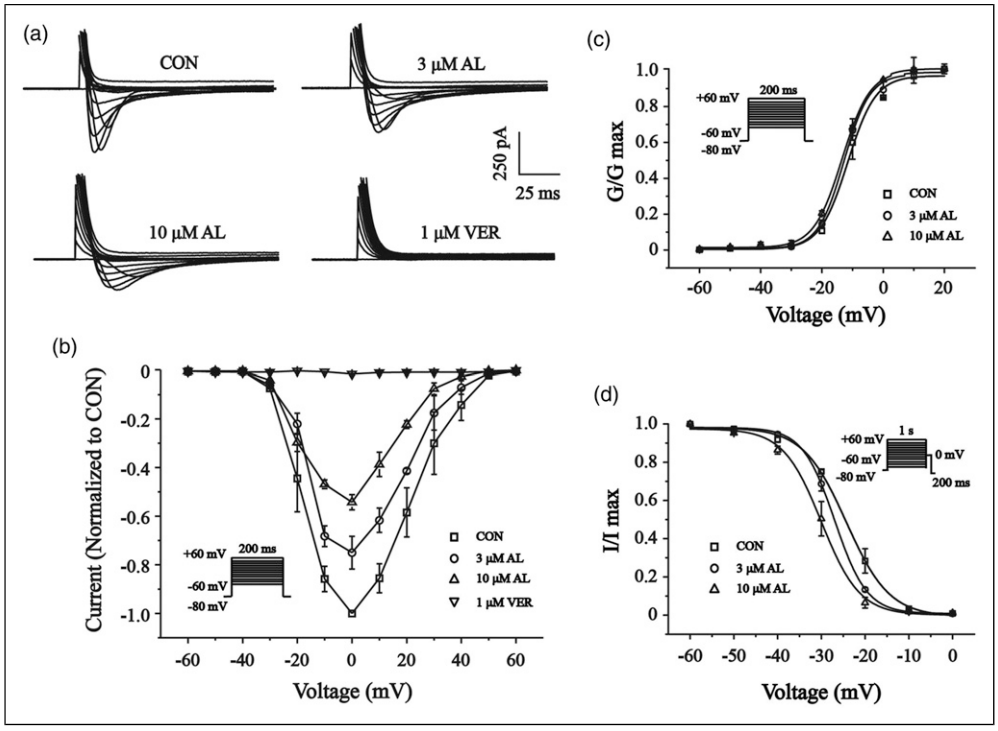

Figure 10. Effects of AL on the dynamical properties of the Ca^{2+} channel. (a) Representative $I_{Ca\text{-}L}$ in the CON, AL (3, 10 μM), or VER (1 μM) conditions logged according to the steady-state activation protocol. (b) The I-V relationship of $I_{Ca\text{-}L}$ in the absence (□) or presence of 3 μM AL (○), 10 μM AL (△), or 1 μM VER (▽). (c) Activation and (d) inactivation curves from the I-V curves in the absence (□) or presence of 3 μM AL (○), 10 μM AL (△). The values are the means ± SEM (n = 6, $^{\#\#}p < 0.01$ vs CON).

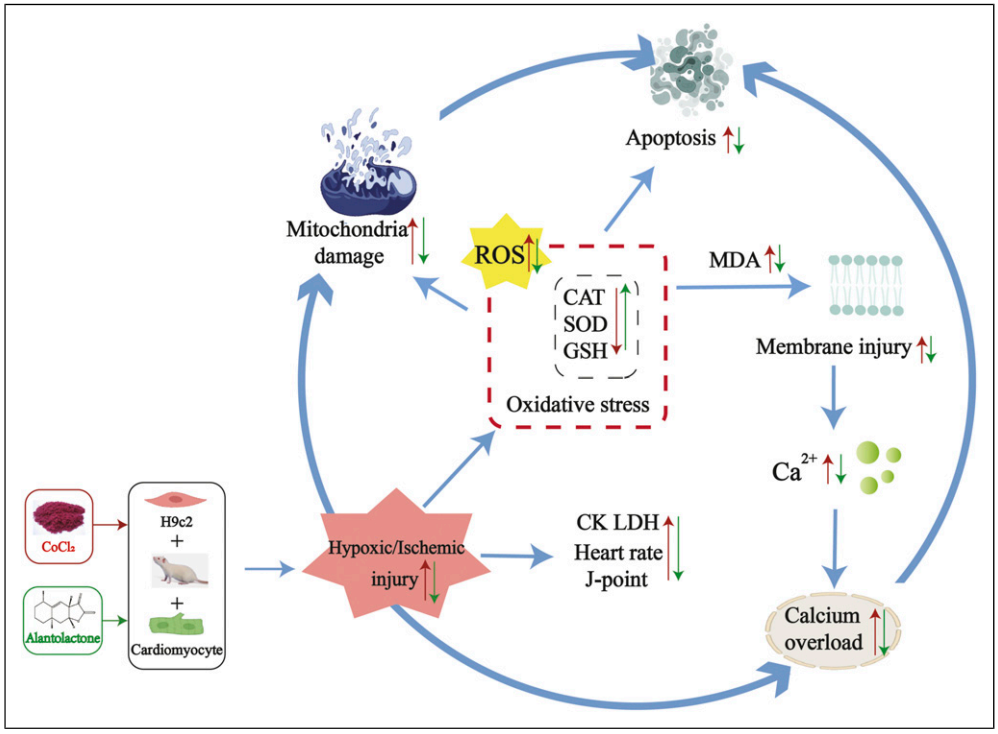

Figure 11. Cardioprotective effects of AL on MI injury.

AL provided a free radical scavenging property. Mammals eliminate ROS using reducing enzymes such as SOD, CAT, and GSH; therefore, concentrations of these "free-radical scavengers" reflect cells' ability to neutralize free radicals and reduce oxidative stress. SOD is one of the primary enzymes used by cells to maintain oxidative homeostasis.[39] GSH is also a major cellular antioxidant that serves not only as a direct electron donor to neutralize H_2O_2 and lipid peroxide, but also the scavenger of oxygen and nitrogen radicals.[40] CAT protects against toxic oxygen metabolites.[41] Under standard conditions, H9c2 cardiomyocytes contain high levels of SOD, CAT, and GSH. However, when cells are exposed to $CoCl_2$-induced H/I injury, these antioxidant defense systems are destroyed, and both the level and concentration of SOD, CAT, and GSH might decrease. Additionally, MDA is the end product of polyunsaturated fatty acids and is often used to evaluate cardiac lipid peroxidation.[42] In the present study, the $CoCl_2$ group had increased MDA content and decreased levels of CAT, SOD, and GSH. However, pretreatment with AL significantly reduced the content of MDA and restored SOD, CAT, and GSH activity. These results suggested that the cardioprotective effect of AL might be attributable to its antioxidative activity.

Myocardial mitochondria are vulnerable to damage induced by ischemia, which can lead to cardiac dysfunction.[43] In the heart, a shift in mitochondrial permeability can result from the mitochondrial dysfunction caused by oxidative stress or other stimuli, a disruption of the MMP.[44] Oxidative stress and the generation of ROS can lead to abnormal mitochondrial function.[45] In this study, the exposure of H9c2 cardiomyocytes to hypoxia led to mitochondrial damage that significantly improved with AL pretreatment.

Excessive ROS disrupt the structure of the cell membrane, increase the permeability of cell membrane, and lead to large amounts of calcium influx from the extracellular environment, resulting in intracellular calcium overload.[46] This ROS-induced increase in Ca^{2+} is a constant feature of pathological states related to oxidative stress.[47] Ca^{2+} released from the sarcoplasmic reticulum through the ryanodine receptor (RyR) also contributes to elevated intracellular Ca^{2+} concentrations. The excessive increase of Ca^{2+} concentration in cells can lead to calcium overload and therefore result in damage to cardiac cells.[48] Preventing the rise in intracellular Ca^{2+} concentration could reduce cardiac damage.[49] To detect the accumulation of Ca^{2+} in cells after hypoxia/ischemia-induced, the fluorescence intensity of Ca^{2+} marked by Fluo-3/AM was observed under a confocal microscope. As shown in Figure 6, exposure of H9c2 cells to H/I conditions resulted in a significant increase in intracellular Ca^{2+} fluorescence indicated by Fluo-3/AM. Pretreatment with AL attenuated this fluorescence intensity. Our results suggest that AL can alleviate calcium overload in H9c2 cells.

Since Ca^{2+} cannot be degraded, Ca^{2+} levels can only be controlled by transporting the ions across membranes. There are three potential sources of Ca^{2+} entry: (1) LTCCs.[50] (2) sarcoplasmic Na^+/Ca^{2+} exchanger.[51] (3) another calcium entry pathway.[52] Calcium influx is predominantly carried out by LTCCs in cardiac cells. LTCCs play a central role in calcium overload, and the regulation of LTCC activity is the focus of considerable research efforts.[53] The inhibition of LTCCs leads to a decrease in Ca^{2+} entry, which in turn reduces harmful calcium overload, thereby protecting the heart against ischemic injury. Calcium ion blockers are the most common and widely used drugs for the treatment of MI. Therefore, the effects of AL on LTCCs in isolated rat ventricular myocytes were investigated using the whole-cell patch-clamp technique. In these experiments, VER was used as the positive control to block the LTCCs.[54] Our data suggest that AL reduces $I_{Ca\text{-}L}$ in a concentration-dependent manner with an IC_{50} of 17.29 μmol/L in cardiomyocytes. AL also reduced $I_{Ca\text{-}L}$ at 10 μmol/L in both healthy and ischemic myocardial cells. Figure 10 shows that neither the reversal potential nor the I-V relationship of $I_{Ca\text{-}L}$ changed. Furthermore, at 3 and 10 μmol/L, AL shifted the steady-state activation and inactivation curves of $I_{Ca\text{-}L}$ to the left. These results demonstrate that MI suppressed the $I_{Ca\text{-}L}$ primarily by decreasing the Ca^{2+} current amplitude, a component of the mechanism underlying AL's effects against MI injury.

One of the limitations of this study is that there is a gap between this experimental environment and the physiological environment of cardiomyocytes. Furthermore, in this study, AL inhibits Ca^{2+} inflow by suppressing gated voltage LTCCs, thus alleviate intracellular calcium overload and oxidative stress. However, cardiac LTCCs are regulated by a variety of neurotransmitters, hormones, and cytokines. Sperelakis and Schneider demonstrated that β-adrenergic receptor-mediated stimulation of cardiac LTCCs was due to phosphorylation of the channel by cAMP-dependent protein kinase A (PKA).[55] In addition, other signaling pathways have also been suggested to regulate the channel by phosphorylation. α-Adrenergic agonists, endothelin, and angiotensin II all regulate LTCCs through the protein kinase C (PKC) pathway.[56,57] Thus, additional studies are needed to identify the pathways underlying AL's impact in MI. Furthermore, whether AL acts directly on ISO (e.g. by degrading it) must be addressed in future studies on the relationship between the AL and ISO.

Conclusions

In a nutshell, the overall findings exemplify that AL alleviates cardiac injury in vivo and in vitro. The cardioprotective

effects of AL may be related to decreased heart rate, ST interval, and alleviated myocardial pathological injury. Meanwhile, as shown in Figure 11, AL protects H9c2 cells against $CoCl_2$-induced H/I injury by improving cell viability, apoptosis, LDH, and CK leakage, antioxidant defenses, mitochondrial damage, and calcium overload. In addition, our findings support that, as an LTCC blocker, AL may play a positive role in the protection of ischemic cardiomyopathy.

Declaration of conflicting interests

The author(s) declared no potential conflicts of interest with respect to the research, authorship, and/or publication of this article.

Funding

The author(s) disclosed receipt of the following financial support for the research, authorship, and/or publication of this article: This work was sponsored by grants from the Foundation of Medical Science Research of Hebei Province (No. 20180886).

Ethical approval

Ethical approval for this study was obtained from the Ethics Committee for Animal Experiments of Hebei University of Chinese Medicine (approval number: DWLL2020073).

Informed consent

There are no human subjects in this article and informed consent is not applicable.

Animal welfare

The present study followed international, national, and/or institutional guidelines for humane animal treatment and complied with relevant legislation.

Availability of data and materials

The datasets used or analyzed during the current study are available from the corresponding author on reasonable request.

Statement of human and animals rights

All experimental procedures with animal subjects in this study were conducted in accordance with the Guidelines of Animal Experiments from the Committee of Medical Ethics.

ORCID iDs

Yangshuang Liu https://orcid.org/0000-0001-5537-9626
Li Chu https://orcid.org/0000-0002-6301-2709

References

1. Ma X, Zhang K, Li H, Han S, Ma Z and Tu P (2013) Extracts from Astragalus membranaceus limit myocardial cell death and improve cardiac function in a rat model of myocardial ischemia. *Journal of Ethnopharmacology* 149(3): 720–728.
2. Tu G, Zou L, Liu S, et al. (2020) Correction to: long noncoding NONRATT021972 siRNA normalized abnormal sympathetic activity mediated by the upregulation of P2X7 receptor in superior cervical ganglia after myocardial ischemia. *Purinergic Signalling* 16(4): 603–604.
3. Dhalla N, Elmoselhi AB, Hata T and Makino N (2000) Status of myocardial antioxidants in ischemia-reperfusion injury. *Cardiovascular Research* 47(3): 446–456.
4. Kaminski KA, Bonda TA, Korecki J and Musial WJ (2002) Oxidative stress and neutrophil activation-the two keystones of ischemia/reperfusion injury. *International Journal of Cardiology* 86(1): 41–59.
5. Jiang Q, Yu T, Huang K, Zhang H, Zheng Z and Hu S (2018) Systemic redistribution of the intramyocardially injected mesenchymal stem cells by repeated remote ischaemic postconditioning. *Journal of Cellular and Molecular Medicine* 22(1): 417–428.
6. Dröge W (2002) Free radicals in the physiological control of cell function. *Physiological Reviews* 82(1): 47–95.
7. Braunersreuther V and Jaquet V (2012) Reactive oxygen species in myocardial reperfusion injury: from physiopathology to therapeutic approaches. *Current Pharmaceutical Biotechnology* 13(1): 97–114.
8. Bersohn MM, Morey AK and Weiss RS (1997) Sarcolemmal calcium transporters in myocardial ischemia. *Journal of Molecular and Cellular Cardiology* 29(9): 2525–2532.
9. Zhao D and Dhalla NS (1989) Influence of gramicidin S on cardiac membrane Ca2+/Mg2+ ATPase activities and contractile force development. *Canadian Journal of Physiology and Pharmacology* 67(6): 546–552.
10. Bers DM (2008) Calcium cycling and signaling in cardiac myocytes. *Annual Review of Physiology* 70: 23–49.
11. Satoh H and Horie M (1997) Actions of taurine on the L-Type Ca2+ channel current in guinea pig ventricular cardiomyocytes. *Journal of Cardiovascular Pharmacology* 30(6): 711–716.
12. Zhao Z, Liu M, Zhang Y, et al. (2020) Cardioprotective effect of monoammonium glycyrrhizinate injection against myocardial ischemic injury in vivo and in vitro: involvement of inhibiting oxidative stress and regulating Ca^{2+} homeostasis by L-type calcium channels. *Drug Design, Development and Therapy* 14: 331–346.
13. Misra MK, Sarwat M, Bhakuni P, Tuteja R and Tuteja N (2009) Oxidative stress and ischemic myocardial syndromes. *Medical Science Monitor: International Medical Journal of Experimental and Clinical Research* 15(10): RA209–219.
14. Takimoto E and Kass DA (2007) Role of oxidative stress in cardiac hypertrophy and remodeling. *Hypertension* 49(2): 241–248.
15. Han D, Ybanez MD, Johnson HS, et al. (2012) Dynamic adaptation of liver mitochondria to chronic alcohol feeding in mice. *Journal of Biological Chemistry* 287(50): 42165–42179.

16. Schriner SE, Linford NJ, Martin GM, et al. (2005) Extension of murine life span by overexpression of catalase targeted to mitochondria. *Science* 308(5730): 1909–1911.
17. Simon H-U, Haj-Yehia A and Levi-Schaffer F (2000) Role of reactive oxygen species (ROS) in apoptosis induction. *Apoptosis* 5(5): 415–418.
18. de Groot H (1994) Reactive oxygen species in tissue injury. *Hepato-Gastroenterology* 41(4): 328–332.
19. Ansari J, Kaur G and Gavins FNE (2018) Therapeutic potential of annexin A1 in ischemia reperfusion injury. *International Journal of Molecular Sciences* 19(4): 1211.
20. Schaper J, Meiser E and Stämmler G (1985) Ultrastructural morphometric analysis of myocardium from dogs, rats, hamsters, mice, and from human hearts. *Circulation Research* 56(3): 377–391.
21. Wahab A, Gao K, Jia C, et al. (2017) Significance of resveratrol in clinical management of chronic diseases. *Molecules* 22(8): 1329.
22. Dang X, He B, Ning Q, et al. (2020) Alantolactone suppresses inflammation, apoptosis and oxidative stress in cigarette smoke-induced human bronchial epithelial cells through activation of Nrf2/HO-1 and inhibition of the NF-κB pathways. *Respiratory Research* 21(1): 95.
23. Ojha S, Nandave M, Kumaria S and Arya DS (2010) Cardioprotection by Inula racemosa Hook in experimental model of myocardial ischemic reperfusion injury. *Indian Journal of Experimental Biology* 48(9): 918–924.
24. Monasky MM, Varian KD and Janssen PML (2008) Gender comparison of contractile performance and beta-adrenergic response in isolated rat cardiac trabeculae. *Journal of Comparative Physiology B* 178(3): 307–313.
25. Sahyoun HA and Hicks R (1981) Abnormal electrocardiographic activity revealed by isolated rat heart preparations at various times after experimental myocardial infarction. *Cardiovascular Research* 15(3): 144–150.
26. Grimm D, Elsner D, Schunkert H, et al. (1998) Development of heart failure following isoproterenol administration in the rat: role of the renin-angiotensin system. *Cardiovascular Research* 37(1): 91–100.
27. Shi YN, Zhang XQ, Hu ZY, et al. (2019) Genistein protects H9c2 cardiomyocytes against chemical hypoxia-induced injury via inhibition of apoptosis. *Pharmacology* 103(5–6): 282–290.
28. Qu C, Xu D-Q, Yue S-J, et al. (2020) Pharmacodynamics and pharmacokinetics of Danshen in isoproterenol-induced acute myocardial ischemic injury combined with Honghua. *Journal of Ethnopharmacology* 247: 112284.
29. Van Acker H, Gielis J, Acke M, Cools F, Cos P and Coenye T (2016) The role of reactive oxygen species in antibiotic-induced cell death in burkholderia cepacia complex bacteria. *PLoS One* 11(7): e0159837.
30. Wang Y, Li X, Zhang X, Song JQ, Kang Y and Lou JS (2012) The protective effect of the Guanxinsuhe capsules serum on hydrogen peroxide injured cardiocytes of neonate rat. *Pharmacology in Clinical Chinese Materials Medicine* 28(3).
31. Hao D, Li X, Kang L, et al (2012) Effect of Guanxin Suhe capsule on cTn-T and myocardial enzyme in rat acute myocardial infarction. *Chinese Journal of Experimental Traditional Medical Formulae* 18(23): 195–199.
32. Cadenas S (2018) ROS and redox signaling in myocardial ischemia-reperfusion injury and cardioprotection. *Free Radical Biology and Medicine* 117: 76–89.
33. Pagliaro BR, Cannata F, Stefanini GG and Bolognese L (2020) Myocardial ischemia and coronary disease in heart failure. *Heart Failure Reviews* 25(1): 53–65.
34. Ferrans VJ, Hibbs RG, Black WC and Weilbaecher DG (1964) Isoproterenol-induced myocardial necrosis. A histochemical and electron microscopic study. *American Heart Journal* 68: 71–90.
35. Leonardi F, Passeri B, Fusari A, et al. (2008) Cardiac Troponin I (cTnI) concentration in an ovine model of myocardial ischemia. *Research in Veterinary Science* 85(1): 141–144.
36. Hescheler J, Meyer R, Plant S, Krautwurst D, Rosenthal W and Schultz G (1991) Morphological, biochemical, and electrophysiological characterization of a clonal cell (H9c2) line from rat heart. *Circulation Research* 69(6): 1476–1486.
37. Liu YC, Wang YJ and Wu SN (2008) The mechanisms of propofol-induced block on ion currents in differentiated H9c2 cardiac cells. *European Journal of Pharmacology* 590(1–3): 93–98.
38. Ding Z-M, Jiao X-F, Wu D, et al. (2017) Bisphenol AF negatively affects oocyte maturation of mouse in vitro through increasing oxidative stress and DNA damage. *Chemico-Biological Interactions* 278: 222–229.
39. Liu J, Hou J, Xia ZY, et al. (2013) Recombinant PTD-Cu/Zn SOD attenuates hypoxia-reoxygenation injury in cardiomyocytes. *Free Radical Research* 47(5): 386–393.
40. Leichtweis S and Ji LL (2001) Glutathione deficiency intensifies ischaemia-reperfusion induced cardiac dysfunction and oxidative stress. *Acta Physiologica Scandinavica* 172(1): 1–10.
41. Ferrari R, Ceconi C, Curello S, Cargnoni A, Condorelli E and Raddino R (1985) Role of oxygen in myocardial ischaemic and reperfusion damage: effect of alpha-tocopherol. *Acta Vitaminologica et Enzymologica* 7(suppl): 61–70.
42. Wei B, Li W-W, Ji J, Hu Q-H and Ji H (2014) The cardioprotective effect of sodium tanshinone IIA sulfonate and the optimizing of therapeutic time window in myocardial ischemia/reperfusion injury in rats. *Atherosclerosis* 235(2): 318–327.
43. Zhang C-X, Cheng Y, Liu D-Z, et al. (2019) Mitochondria-targeted cyclosporin A delivery system to treat myocardial ischemia reperfusion injury of rats. *Journal of Nanobiotechnology* 17(1): 18.
44. Kovácsová B, Pazin-Hricková E, Csabáková L and Svec P (1994) [The effect of butylhydroxyanisole, an antioxidant,

on oxidative phosphorylation of myocardial mitochondria in experimental ischemia]. *Ceska a Slovenska Farmacie: Casopis Ceske Farmaceuticke Spolecnosti a Slovenske Farmaceuticke Spolecnosti* 43(1): 18–21.

45. Lesnefsky EJ, Tandler B, Ye J, Slabe TJ, Turkaly J and Hoppel CL (1997) Myocardial ischemia decreases oxidative phosphorylation through cytochrome oxidase in subsarcolemmal mitochondria. *The American Journal of Physiology* 273(3 Pt 2): H1544–H1554.
46. Zhu P, Hu S, Jin Q, et al. (2018) Ripk3 promotes ER stress-induced necroptosis in cardiac IR injury: a mechanism involving calcium overload/XO/ROS/mPTP pathway. *Redox Biology* 16: 157–168.
47. Nicotera P, McConkey D, Svensson SA, Bellomo G and Orrenius S (1988) Correlation between cytosolic Ca2+ concentration and cytotoxicity in hepatocytes exposed to oxidative stress. *Toxicology* 52(1–2): 55–63.
48. Kasai H, Yao A, Oyama T, et al. (2004) Direct measurement of Ca2+ concentration in the SR of living cardiac myocytes. *Biochemical and Biophysical Research Communications* 314(4): 1014–1020.
49. Li Q, Cui N, Du Y, Ma H and Zhang Y (2013) Anandamide reduces intracellular Ca2+ concentration through suppression of Na+/Ca2+ exchanger current in rat cardiac myocytes. *PLoS One* 8(5): e63386.
50. Striessnig J, Pinggera A, Kaur G, Bock G and Tuluc P (2014) L-type Ca 2+ channels in heart and brain. *Wiley Interdisciplinary Reviews: Membrane Transport and Signaling* 3(2): 15–38.
51. Kappl M and Hartung K (1996) Rapid charge translocation by the cardiac Na(+)-Ca2+ exchanger after a Ca2+ concentration jump. *Biophysical Journal* 71(5): 2473–2485.
52. Csutora P, Zarayskiy V, Peter K, et al. (2006) Activation mechanism for CRAC current and store-operated Ca2+ entry. *Journal of Biological Chemistry* 281(46): 34926–34935.
53. Wang L, Lei Q, Zhao S, et al. (2020) Ginkgolide B maintains calcium homeostasis in hypoxic hippocampal neurons by inhibiting calcium influx and intracellular calcium release. *Frontiers in Cellular Neuroscience* 14: 627846.
54. Li W and Shi G (2019) How CaV1.2-bound verapamil blocks Ca2+ influx into cardiomyocyte: atomic level views. *Pharmacological Research* 139: 153–157.
55. Sperelakis N and Schneider JA (1976) A metabolic control mechanism for calcium ion influx that may protect the ventricular myocardial cell. *The American Journal of Cardiology* 37(7): 1079–1085.
56. Calderón-Sánchez EM, Ávila-Medina J, Callejo-García P, Fernández-Velasco M, Ordóñez A and Smani T (2020) Role of Orai1 and L-type CaV1.2 channels in Endothelin-1 mediated coronary contraction under ischemia and reperfusion. *Cell Calcium* 86: 102157.
57. Guo X, Chen M, Zeng H, et al. (2018) Quercetin attenuates ethanol-induced iron uptake and myocardial injury by regulating the angiotensin II-L-type calcium channel. *Molecular Nutrition & Food Research* 62(5).